ADVANCES IN LIFELINE EARTHQUAKE ENGINEERING

Thomas D. O'ROURKE[1], Yu WANG[2], and Peixin SHI[2]

SUMMARY

Advances in lifeline earthquake engineering are driven increasingly by sophisticated simulations of system performance to assess service reliability and the regional economic and community impact of damage. This paper provides an overview of factors that affect lifeline system performance, and shows how they are interrelated to provide a framework for developing decision support tools. The paper explores the relationship between component behavior and system performance, and illustrates how system reliability is modeled to quantify improvements derived from retrofitting critical components in water distribution and electric power networks. Methods for modeling the regional economic impact of earthquake damage to lifelines are discussed and illustrated with respect to water distribution and electric power networks.

INTRODUCTION

Lifelines are grouped into six principal systems: electric power, gas and liquid fuels, telecommunications, transportation, waste disposal, and water supply [1]. Taken individually, or in aggregate, these systems are intricately linked with the economic well-being, security, and social fabric of the communities they serve.

The field of lifeline earthquake engineering, and more broadly of lifeline systems, can be viewed in an evolutionary context. Early studies were focused on component behavior and simple system models. They were stimulated in large measure by the effects of individual earthquakes on transportation, water delivery, and electric power facilities. As more advanced experimental and computational modeling was developed, network simulations were explored to assess system reliability. Most recently, the economic and community consequences of earthquake damage have been integrated with system simulations to create models and a modeling process that link component behavior through system reliability assessments all the way to regional economic impact.

As the field has evolved, it has become increasingly more diverse and multidisciplinary in terms of the expertise and interactions that are needed for reliable modeling and for comprehensive support of the decision making process. As the intellectual framework and methodologies have developed for the seismic performance of lifelines, it has become clear that both the process and specific applications are

---

[1] Professor, Cornell University, Ithaca, NY 14853
[2] Graduate Research Assistant, Cornell University, Ithaca, NY 14853

transferable to other hazards, including natural and anthropogenic ones. In fact, recent studies of lifeline system response to the World Trade Center Disaster [2] have emphasized the remarkable degree of interdependence that exists among lifeline systems. An increasing number of investigators [3, 4] recommend that procedures be developed for quantifying and managing the interactions among different lifeline systems. The investigation of such interdependencies has been a cornerstone of lifeline earthquake engineering research and modeling. Hence, there is considerable benefit to be derived from lifeline earthquake engineering for improving the security of civil infrastructure against natural hazards as well as major accidents and premeditated acts of violence.

This paper presents a framework for assessing lifeline system response to earthquakes. Although the concepts and procedures treated in the paper are relevant for all lifeline systems, emphasis is placed on water, fuel, and electric power distribution networks. Using the framework for lifeline system assessment, the paper explores various aspects of system performance and modeling, starting with empirical, analytical, and experimental models for components. It then examines the spatial variability of strong ground motion to help quantify uncertainties with respect to the behavior of many geographically distributed components. Finally, the paper provides an overview of how the larger effects of lifeline system performance are being evaluated in context of community impact and regional economic consequences.
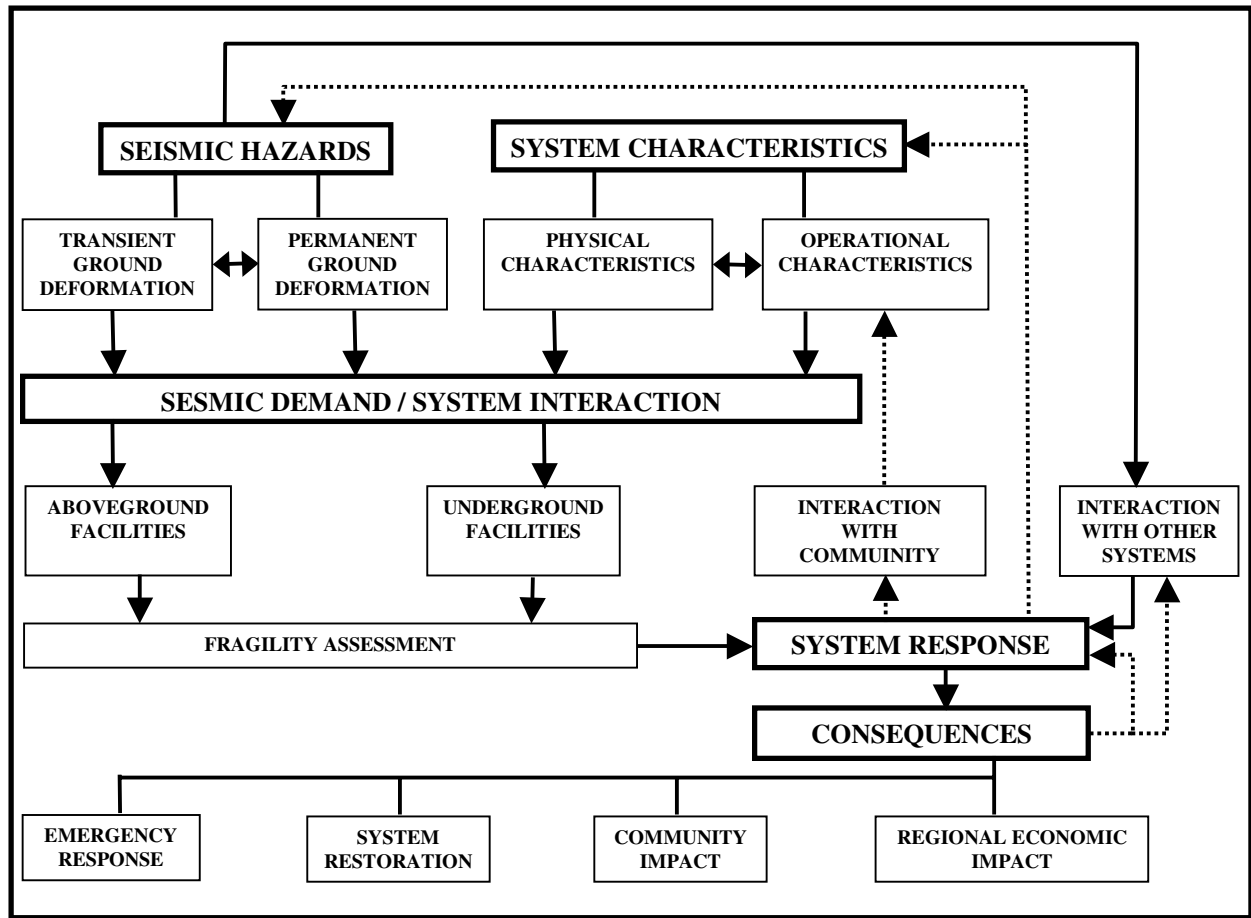
FRAMEWORK FOR EARTHQUAKE EFFECTS ON LIFELINES

Resilience has been proposed as a unifying concept for categorizing the activities necessary to reduce seismic risk and for quantifying measures that enhance a community's ability to prepare for and respond to earthquakes [5]. Given the strong influence of lifelines on the economic capacity, security, and social fabric of communities, these systems play a critical role in building community resilience. A framework for evaluating lifeline response under earthquake effects, therefore, needs to incorporate the technical, organizational, social, and economic dimensions of the system and its operation.

A framework for evaluating lifeline system performance is shown schematically in Fig. 1. Seismic hazards are combined with system characteristics in models that account for the effects of transient ground motion and permanent ground deformation on both aboveground and underground facilities. Fragility analyses of system components are used to assess the overall system response, from which the consequences with respect to the broader community of lifeline users are derived. Interaction with other external systems affects the response of the specific system being evaluated. By setting performance goals with respect to consequences, one can determine the desired level of system response. This response is achieved through interaction with the community by altering operational and physical characteristics of the system, as well as mitigating seismic hazards.

There is a basic chain of activities that predominates in this framework. The basic chain starts with the characterization of seismic hazards and system properties, then proceeds to the analyses of interactions between them, from which system response and the evaluation of community impacts follow. This basic chain is emphasized in Fig. 1 with bold and enlarged print, and its principal features are discussed under the subheadings that follow.

Seismic Hazards

Seismic hazards are grouped into transient and permanent ground deformation (TGD and PGD, respectively). For lifeline systems, TGD includes the strong motion characteristics needed for structural and secondary system response of buildings and aboveground facilities. It also includes factors that influence geographically distributed networks, such as site response, near source and forward directivity effects of fault rupture, sedimentary basin and valley effects, ridge shattering, and ground oscillation

Figure 1   Framework for Lifeline System Performance Under Earthquake Effects

triggered by soil liquefaction [1, 6]. The main sources of PGD include surface faulting, landslides, and soil liquefaction [1]. It has long been realized that the most serious damage to underground lifelines during an earthquake is caused by PGD. Many lifeline systems have substantial numbers of pipelines and conduits (e.g., water supply, gas and liquid fuel, electric power) as well as embankments and tunnels (e.g., transportation and water supply) where performance is linked directly to irrecoverable ground movements. Hence, a distinguishing feature of evaluating lifeline system response to an earthquake is the emphasis that must be placed on PGD.

System Characteristics

System characteristics involve both physical and operational attributes. As indicated in Fig. 2, physical characteristics involve components that must operate under conditions of connectivity, support functional requirements, and interact with the components of both their own and other systems. In crowded urban environments, the failure of an underground component may affect the performance of an adjacent one in another system. Damage can rapidly cascade, for example, from a water main failure to the disruption of nearby fiber optic cables and electric power facilities.

The operational characteristics of the system include its organizational and social aspects. Those who operate the system are the interface for interaction with user communities. Operations in the proposed framework include planning, mapping, monitoring, maintenance and procedures for running the system. Geographical information systems (GIS) are frequently part of the mapping process. However, GIS is much more than a mapping process; it is a means of visualizing system performance and of identifying

```
┌─────────────────────────────────────────────────────────────────────────┐
│                     SYSTEM CHARACTERISTICS                                │
│  PHYSICAL CHARACTERISTICS          OPERATIONAL CHARACTERISTICS            │
│        • COMPONENTS                      • PLANNING                        │
│        • CONNECTIVITY                    • MAPPING AND GIS                 │
│        • FUNCTIONALITY                   • MONITORING                      │
│        • INTERACTION                     • MAINTENANCE                     │
│                                          • OPERATING PROCEDURES            │
└─────────────────────────────────────────────────────────────────────────┘
```

Figure 2   Physical and Operational Characteristics of Lifeline Systems

and quantifying multi-dimensional interactions within a two-dimensional surrogate of the real world.

Seismic Demand / System Interaction

The effects of TGD and PGD are evaluated for the components of aboveground and underground facilities. To account for uncertainty with respect to component or facility response, seismic behavior is frequently characterized by fragility curves that provide the probability of failure as a function of the demand (e.g., peak acceleration, velocity) and confidence limit. Multiple fragility assessments are combined when simulating system response. Typically, Monte Carlo techniques are employed to quantify uncertainty with respect to system-wide behavior.

System Response

System response is evaluated and used as the basis for changing network characteristics and/or mitigating seismic hazards. In some cases, seismic hazards can be reduced by densification of loose, saturated sand deposits, which are vulnerable to liquefaction, and by dewatering and stabilizing areas subject to landslides. Changes in the system characteristics may involve retrofitting existing facilities or replacing components with more resilient ones. Conventional engineering investigations lead to products that perform at a quantifiably improved level. To understand the ramifications of such improvements, simulations of system response must be performed with the improved component characteristics to show how the overall reliability is increased and broader community impacts are reduced.

Consequences

The economic and social impacts of lifeline system disruption are generally the most important with respect to community well-being. The evaluation of system performance needs to incorporate larger social and economic effects to provide a realistic assessment of true expenses. Studies have shown that a strong case for the cost effectiveness of mitigation can generally be made only if the broader economic impacts are determined and accounted for [7].

Interdependencies

Lifeline systems are interdependent, both by virtue of physical proximity and operational interaction. The damage and disruption of seismic hazards in other systems may, in turn, affect the system being assessed. Hence, a key component of the framework is the interaction of the system under scrutiny with other lifeline systems.

In the remaining portions of this paper, four aspects of system performance and characterization are explored. First, component behavior and modeling requirements are illustrated by means of the earthquake behavior of jointed concrete cylinder pipelines (JCCP), which are important components of North America water supply systems. Next, contributions of large-scale experimentation are reviewed with respect to PGD effects on steel gas main performance at elbows. The spatial distribution of strong ground

motion is discussed, and a method for characterizing the spatial variability of its effects on water distribution networks is described. Finally, recent advances in assessing the consequences of lifeline system response in terms of community and regional impacts are reviewed for water and electric power distribution networks.

CHARACTERIZING COMPONENT PERFORMANCE

Performance Overview

The earthquake performance of a lifeline system is often closely related to the performance of a lifeline component. Consider, for example, a particular class of pipelines used for trunk and transmission facilities in North America, referred to collectively in this paper as jointed concrete cylinder pipelines (JCCP). The performance of JCCPs during previous earthquakes has varied significantly, depending on their structural and joint characteristics and on the location and nature of the TGD and PGD they were subjected to. Ayala and O'Rourke [8] reported significant repairs in JCCPs after 1979 Guerrero and 1985 Michoacan earthquakes. Repairs were concentrated at the joints of the trunk and transmission pipelines, and were especially severe for the 1985 Michoacan earthquake. Damage to JCCP trunk lines after the 1994 Northridge earthquake was also high. Lund [9] reported that significant damage was sustained by 1370-mm- and 838-mm- diameter JCCP trunk lines in the Santa Clarita Valley at welded compound bends and as pullout of rubber gasket joints on long horizontal reaches. He further reported that there were 15-20 major pulled joints on a 1980-mm-diameter JCCP trunk line in Simi Valley. In all cases, there is strong evidence that significant damage was caused by TGD.
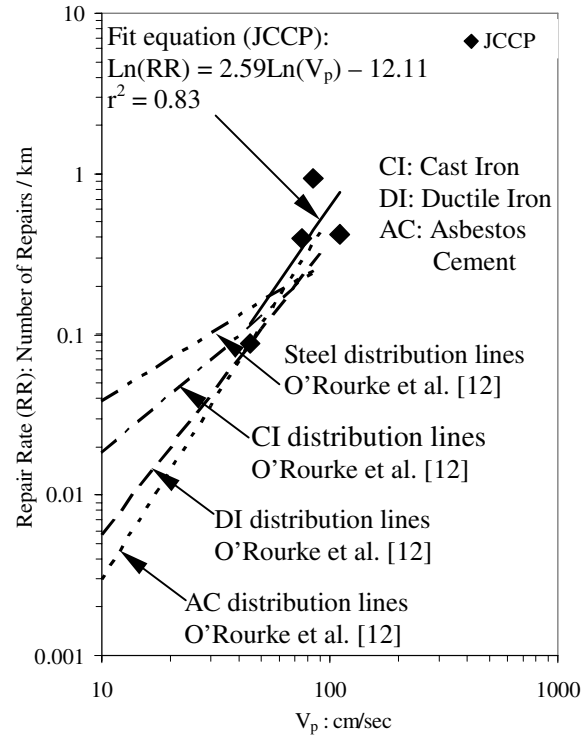
Figure 3 shows a photo of a repaired JCCP that was damaged in the Santa Clarita water supply during the Northridge earthquake. The most vulnerable location in a JCCP is the rubber-gasket bell-and-spigot joint [10], which connects adjoining pipe sections that vary generally from 3 to 8 m in length. The axial tensile capacity of the joint depends on the tensile strength of the poured mortar connection and pullout resistance of the gasket, both of which are relatively low. Moreover, it is not uncommon for the mortar at these joints to be cracked and separated as a result of forces induced during installation or in response to subsequent operational loads and movements in the field.

One method for estimating pipeline damage in future earthquakes is to develop regressions between observed repair rates during previous earthquakes and measured seismic parameters. O'Rourke et al. [10] explain how empirical data were collected about JCCP repairs and locations of repairs after the Northridge earthquake. The geographical coordinates of the repairs and JCCPS were incorporated in a large geographic information system (GIS) database, consisting of over 12,000 km of pipelines and more than 230 strong motion records. Using the GIS database, repair rates (repairs/km) were calculated for areas affected by various levels of peak ground velocity (V_p). Where possible, pipeline repairs in zones of documented PGD were screened from the repair rates so that the resulting statistics would reflect principally the effects of seismic waves or TGD. Figure 4 shows the linear regressions of pipeline repair rate versus V_p. Regressions were developed for V_p because this seismic parameter has been shown to be the most statistically significant one influencing TGD-related pipeline repairs [11]. The figure shows the linear regression for JCCP relative to regressions developed for various types of distribution pipelines by O'Rourke et al. [12] and O'Rourke and Jeon [11].

Whereas the empirical model for JCCP in Fig. 4 can be used for a first order estimate of future earthquake effects, it is limited by the relatively few data acquired for this type of component. In a situation like this, it is useful to develop an analytical model that can expand on the empirically-based predictions and provide insight about soil-structure interaction.

Figure 3   JCCP and Joints
(Photo by D. Ballantyne)

Figure 4   JCCP Repair Rate Correlation
with Peak Ground Velocity, V_p

Model for Seismic Wave Interaction with Pipelines

Figure 5 shows an incremental section of a continuous buried pipeline, dx, subjected a seismic ground wave, simplified as a sinusoidal wave with maximum amplitude of ground strain $\varepsilon_{gmax} = V_p/C$, where V_p is peak ground velocity and C is the apparent wave propagation velocity. The shear transfer between pipe and soil is f, and the pipe axial stiffness is equal to the product of the pipe material modulus, E, and cross-sectional area, A. The rate of pipe strain, ε_p, accumulation is given by

$$\frac{d\varepsilon_p}{dx} = \frac{f}{EA} \tag{1}$$

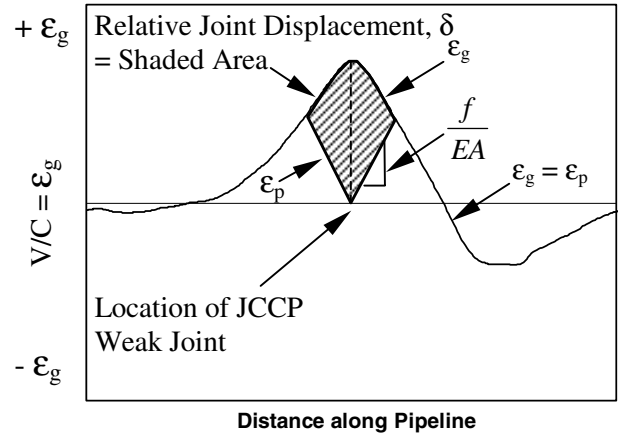The rate of ground strain, ε_g, accumulation is

$$\frac{d\varepsilon_g}{dx} = \frac{d}{dx}(\frac{V}{C}) \tag{2}$$

in which V is the particle velocity. The pipeline is axially flexible with respect to ground strain accumulation if

$$\frac{d\varepsilon_p}{dx} > \frac{d}{dx}(\frac{V}{C}) \tag{3}$$

Figure 5 Sinusoidal Wave Interaction with Pipe Element

Figure 6 Relative Joint Displacement of Flexible Pipeline

This condition should be satisfied everywhere along the pipeline, which requires that $\dfrac{d\varepsilon_p}{dx}$ exceeds the maximum slope $\left(V\!\!\big/\!C\right)_{max}$. For a sinusoidal wave

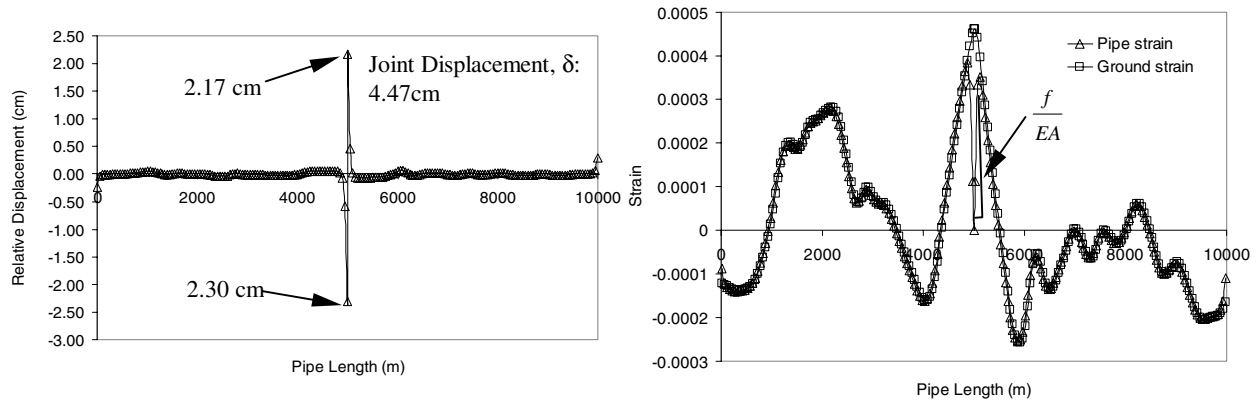$$\left[\frac{d}{dx}\left(\frac{V}{C}\right)\right]_{max} = \frac{2\pi V_p}{\lambda C} \tag{4}$$

in which λ is the wavelength. Combining equations (1) and (4) results in

$$\frac{f}{EA} > \frac{2\pi V_p}{\lambda C} \tag{5}$$

which is the requirement that must be met for a fully flexible pipeline.

   As shown in the figure, another parameter, R, can be defined as the ratio V_p/C to the distance, $\lambda/4$, which can be rapidly discerned from strong motion records. This parameter is used as an index of the seismic wave characteristics, as explained later under the subheading of Finite Element Simulations. Virtually all trunk pipelines are relatively flexible when affected by body waves that have relatively high apparent wave propagation velocities, with the exception of those where soil liquefaction adjacent to the pipelines substantially reduces the shear transfer f. When seismic wave interaction is controlled by surface waves, the wave length can be substantially smaller, in which case the JCCPs may respond as though they were relatively rigid, thus affecting the relative joint displacement.

   Figure 6 illustrates JCCP interaction with seismic ground strain generated by a body wave. Please note that the ground strain, ε_g, is expressed as V/C. Joint displacement during wave interaction is a consequence of variable pullout resistance among the joints in the pipeline. Joints in the field are occasionally cracked and separated due to installation and subsequent ground movement distress. Such joints, being cracked and separated, have very low axial pullout resistance that, for modeling purposes, can be taken as negligible.

(a) Ground-pipeline Relative Displacement   (b) Ground and Pipe Strain

Figure 7   Representative Finite Element Results (O'Rourke et al. [10])

It is assumed that the joints on either side of the cracked joint have full mortar connectivity to mobilize tensile capacity across the joint. Because the pipeline is fully flexible, $\varepsilon_p = \varepsilon_g$ everywhere the pipeline is continuous. At the cracked joint, the pipeline cannot sustain strain, so $\varepsilon_p = 0$. As the wave passes across the cracked joint, strain in the continuous pipeline on each side of the joint will accumulate linearly at a slope of f/EA until $\varepsilon_p = \varepsilon_g$, after which pipe and ground strains are indistinguishable. The shaded area in Fig. 6 represents the integration of the differential strain between the pipeline and ground, which equals the relative joint displacement, δ, that in this case occurs as axial slip.
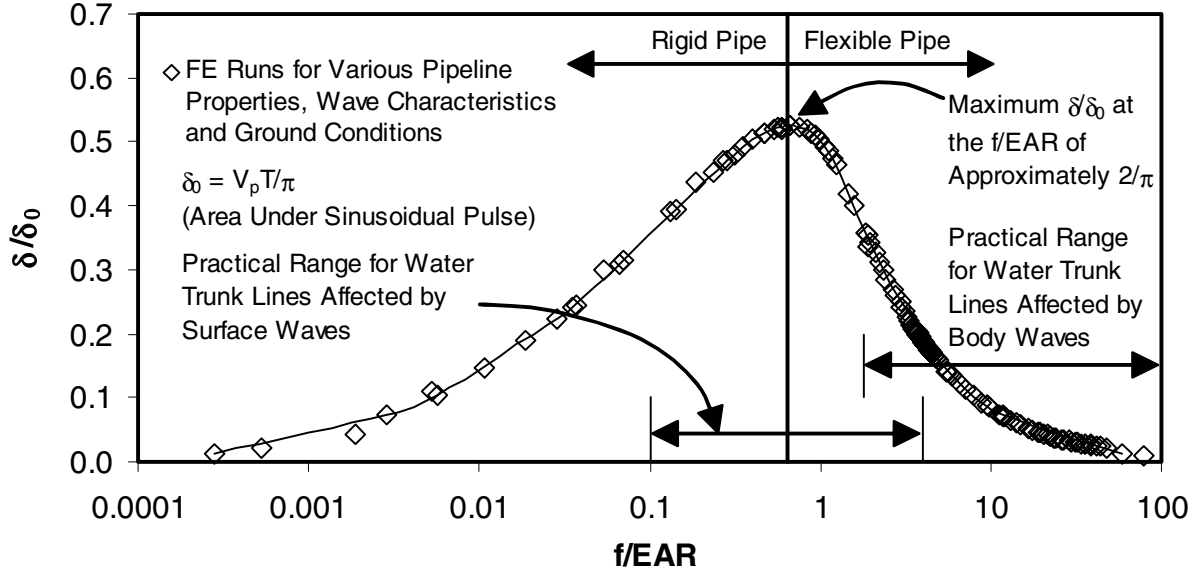
Finite Element Simulations

O'Rourke et al. [10] describe how finite element (FE) analyses were used to evaluate seismic wave interaction with a 1370-mm-diameter PCCP trunk line in Santa Clarita Valley during the Northridge earthquake. Figure 7 shows FE analytical results for a section of pipeline oriented at N23E where there is documented evidence of multiple joint pullouts. The strong motion recording at Newhall Station, approximately 3.5 km from this section of pipeline, was resolved in the direction of the pipeline and used in the analysis. Figure 7a shows the maximum relative joint displacement, which represents pullout for the field condition of wave propagation at this site. The maximum analytical pullout is 4.47 cm, which is distributed somewhat asymmetrically either side of the weak joint to reflect the slightly asymmetric shape of the ground strain pulse. Figure 7b shows the pipe and ground strains on the same plot. It can be seen that, away from the weak joint, $\varepsilon_g = \varepsilon_p$, as is characteristic of a flexible pipeline. The area between the ε_g and ε_p, plotted in the vicinity of the weak joint, represents the relative joint displacement. The FE analytical results show axial joint pullout between 1.0 and 4.5 cm for the various orientations of damaged pipeline relative to the waveform recorded at the Newhall Station. This range of displacement is consistent with pullout of sufficient magnitude to cause leakage and occasional disengagement of the pipeline, as was observed in the field.

The FE model was used to simulate seismic wave interaction for various ground conditions (i.e., soft to stiff clays, lose to dense sands under dry or submerged conditions), pipeline characteristics (i.e., EA combinations and pipe diameters), and seismic wave characteristics (i.e., predominant period, peak ground velocity, and phase velocity for surface waves). In total, 135 FE runs were performed to account for different combinations of ground conditions, pipeline properties, and seismic wave characteristics.

The finite element results are summarized in Fig. 8 with two dimensionless parameters, δ/δ_0 and f/EAR. δ_0 is defined as the area under the seismic sinusoidal ground strain pulse (Fig. 5) and can be calculated by

Figure 8   Universal Relationship Between δ/δ₀ and f/EAR

$$\delta_0 = \int_0^{\lambda/2} \frac{V_p}{C} \sin(\frac{2\pi x}{\lambda}) dx \qquad (6)$$

When combined with

$$\lambda = CT \qquad (7)$$

in which T is predominant period of the seismic wave, δ_0 can be expressed as

$$\delta_0 = \frac{V_p T}{\pi} \qquad (8)$$

The dimensionless parameter, δ/δ_0, is the relative joint displacement normalized with respect to a displacement index of the seismic wave characteristics. The dimensionless parameter, f/EAR, represents a combination of key ground conditions, pipeline properties, and seismic wave characteristics. The shear transfer between soil and pipeline, f, is a function of interface shear strength properties between soil and pipe, pipeline burial depth, and pipe diameter in units of force per length. A procedure to calculate f for pipelines buried in cohesive and cohesionless soils is given by O'Rourke [1]. EA is the axial deformation stiffness of the pipe. As shown in Fig. 5, the seismic wave is characterized by R, which is the ratio of V_p/C to $\lambda/4$.

Figure 8 shows the relationship between δ/δ_0 and f/EAR based on the results from 135 FE simulations. When f/EAR is greater than 100 or less than 0.001, δ/δ_0 approaches 0. The δ/δ_0 increases to a maximum at f/EAR of approximately $2/\pi$, after which it decreases to zero at f/EAR of 100.

Combining the condition expressed by Eqn. 5 and the dimensionless relationship in Fig. 8, a relatively flexible pipeline is defined as one for which

$$\frac{f}{EAR} > \frac{2}{\pi} \qquad\qquad (9)$$

In contrast, a pipeline is considered relatively rigid when

$$\frac{f}{EAR} < \frac{2}{\pi} \qquad\qquad (10)$$

Practical ranges of f/EAR for water trunk lines affected by surface and body waves are also shown in Fig. 8. Water trunk lines tend to behave as relatively flexible pipelines when affected by body waves, and act as relatively rigid pipelines when affected by surface waves.

With known ground conditions, pipeline properties, and seismic wave characteristics, f/EAR and δ_0 can be calculated and joint displacement δ can be estimated directly using Fig.8. Consider, for example, a JCCP with 1575-mm diameter and 157-mm wall thickness subjected to a near source velocity pulse with V_p = 100 cm/sec, C = 2500 m/sec, and T = 1sec. The pipeline is buried at a depth of 1.86 m to the center of pipeline in soil with γ = 18.8 kN/m^3 and φ' = 35°. The EA, R, f, and δ_0 are calculated as 2.7×10^7 kN, 6.4×10^{-7} m^{-1}, 103.9 kN/m, and 31.8 cm, respectively, resulting in f/EAR = 6.0. Using Fig. 8, δ/δ_0 is estimated as 0.135, and the relative joint displacement, δ, is about 4.3 cm. Consider the same pipeline with the same ground conditions, subjected to a seismic surface wave with V_p = 30 cm/sec, phase velocity C = 200 m/sec, and T = 4 sec. R and δ_0 are calculated as 7.5×10^{-6} m^{-1} and 38.2 cm, respectively, resulting in f/EAR = 0.51. Therefore, δ/δ_0 from Fig. 8 is about 0.518, and the relative joint displacement δ is about 19.8 cm. The large predicted displacement for this example indicates a strong potential for joint pullout and disengagement of the pipeline.

The model developed for the joint response of JCCPs to sesmic wave interaction expands greatly on the empirically based model embodied in the regression in Fig.4. By accounting for the mechanism of shear trasfer and relative joint movement during seismic wave interaction, substantial insight about potential joint movement is obtained. The dimensionless plot in Fig. 8 can be applied to virtually all cases of seismic wave interaction with conventional JCCPs. As indicated in the figure and illustrated in the example calculations above, joint pullout can be most severe for surface wave effects. The surfae waves generated by previous earthquakes in lake clay basins in and surrounding Mexio City are examples of the kind of seismic wave interaction that imposes the potentially greatest demand. The observed JCCP performance during the 1979 Guerrero and 1985 Michoacan earthquakes is consistent with the behavoir indicated in Fig. 8. The largest ground strains associated with surface waves are driven by relatively low phase velocities, whereas the largest ground strains associated with body waves are driven by near source velocity pulses.

The model has application to structures other than pipelines. With appropriate modifications to include various levels of resistance to pullout, the model can be used to predict deformation at flexible connections between subaqueous tunnels and shore facilities. For example, recent work to retrofit the Bay Area Rapid Transit System has focused on the potential slip of seismic joints connecting the Transbay Tube with ventilation structures on either side of San Francisco Bay [13]. Concerns about relative joint displacement during seismic wave interaction, similar to those for JCCPs, have a strong influence on the retrofitting requirements for this transporation lifeline.

PGD EFFECTS ON UNDERGROUND LIFELINES

As previously discussed, PGD effects are very important for underground lifelines. Significant work

has been performed in developing models for soil-structure interaction in response to PGD [14]. Moreover, the current generation of commercially available software is capable of simulating pipeline response to PGD well into the nonlinear range of stress versus deformation for both extension and compression. Eidinger et al. [15] report on the deformation of a 2.2-m-diameter welded steel pipeline that was subjected to approximately 3 m of right lateral offset on the Northern Anatolian fault. Pipeline response to fault movement was simulated with the ANSR-III computer program to produce analytical results that compare favorably with the observed deformation pattern and locations of pipeline leakage.

The development and use of increasingly sophisticated programs for soil-structure interaction provide substantial opportunities for characterizing complex lifeline behavior. The models and programs being developed, however, require validation either by comparison through case history studies of analytical results with observed deformation in the field, or by comparison with full-scale laboratory tests that provide detailed measurements of post-yield structural response and soil-pipe interaction.
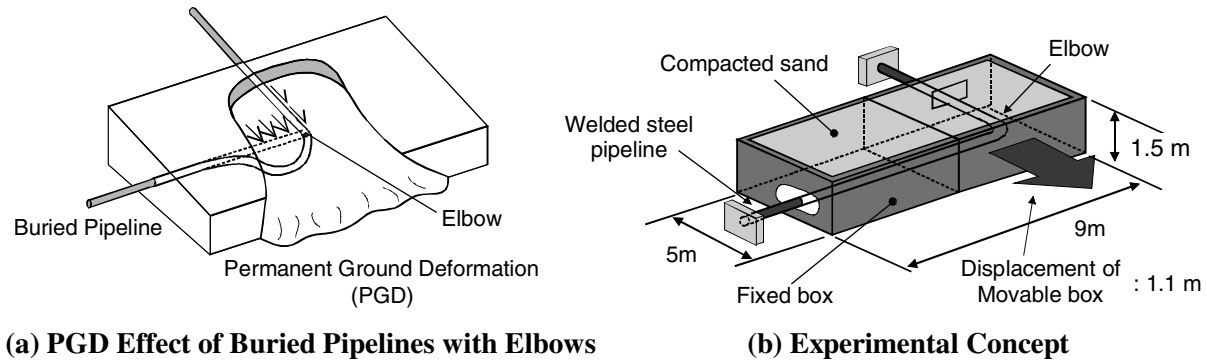
Yoshizaki et al. [16] report on large-scale experiments to evaluate the performance of steel pipelines with elbows subject to PGD. Figure 9 illustrates the concept of the large-scale experiments. A steel pipeline with an elbow is installed under the actual soil, fabrication, and compaction procedures encountered in practice, and then subjected to lateral soil displacement. The scale of the experimental facility is chosen so that large soil movements are generated, inducing soil-pipeline interaction unaffected by the boundaries of the test facility in which the pipeline is buried. The ground deformation simulated by the experiment represents deformation conditions associated with lateral spread, landslides, and fault crossings, and therefore applies to many different geotechnical scenarios. In addition, the experimental data and analytical modeling products are of direct relevance to underground gas, water, petroleum, and electrical conduits.

Only the salient features of these experiments are summarized herein. The experimental pipeline consisted of 100-mm-diameter welded steel pipe with 4.1-mm wall thickness. The pipeline was composed of two straight sections, 5.4 and 9.3-m-long, welded at a 90° elbow. The instrumented pipeline-elbow configuration was constructed and buried in a test compartment, composed of a movable box and fixed box. Each end of the pipeline-elbow configuration was bolted to a reaction wall to simulate upper bond deformation associated with an anchored or locally restrained section of pipeline. The inside dimensions of the L-shaped moveable box were 4.2 × 6 m by 1.5 m deep. The stationary box was 2.4 × 2.7 m by 1.5 m deep. The moveable box was displaced relative to the fixed box along an abrupt vertical plane at the intersection of the two boxes to generate 1 m of right lateral strike slip displacement.
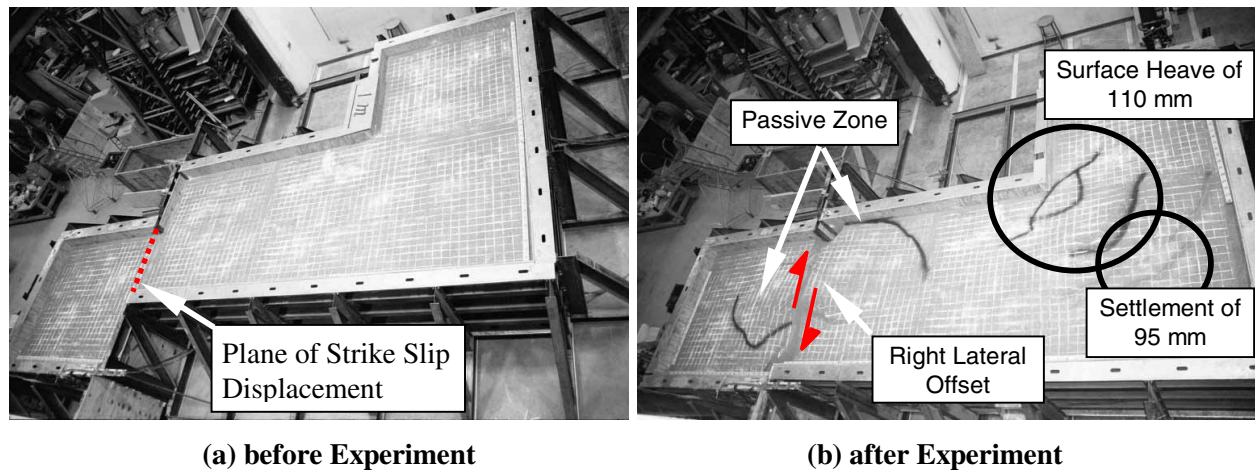
Approximately 60 metric tons of sand were moved from a storage bin to the test compartment for each experiment. Both dry and partially saturated sands were used in the tests, with soil placed and compacted in 150-mm lifts under strict controls on water content and in situ density.

Figure 10 shows the ground surface of the test compartment before and after an experiment. Surficial heaving and settlement are indicated on the figure in the areas near the pipeline elbow and the abrupt displacement plane between the movable and fixed boxes. In all cases, planes of soil slip and cracking reached the ground surface, but did not intersect the walls of the test compartment to any appreciable degree. Leakage occurred at the connection between the elbow and the shorter straight pipe when the ground displacement was 0.78 m. Full circumferential rupture of the pipe occurred when the displacement was 0.94 m.

The large-scale experiments were used to refine and validate a numerical modeling procedure, referred to as the HYBRID MODEL [16], in which the elbow and adjacent portion of the straight pipe sections are modeled with shell elements using the program ABAQUS. The shell elements are linked with

| (a) PGD Effect of Buried Pipelines with Elbows | (b) Experimental Concept |

Figure 9 Experimental Concept for PGD Effects on Buried Pipelines with Elbows
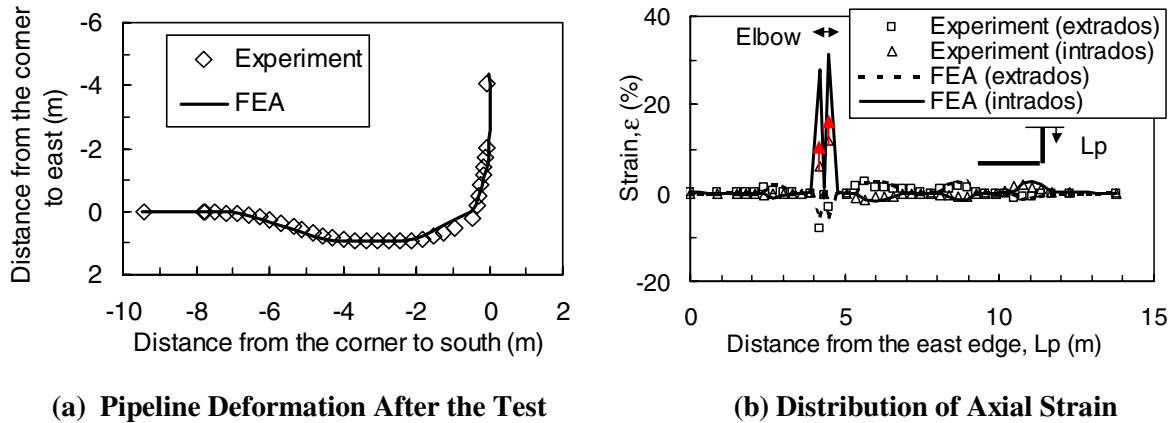

| (a) before Experiment | (b) after Experiment |

Figure 10 Overhead View of Test Compartment Before and After PGD Experiment

beam elements to represent sections of straight pipe outside the zone of large localized strain. Soil-pipeline interaction in response to relative displacement between pipe and soil is modeled with discrete spring elements using a bilinear force-displacement relationship to represent the elasto-plastic nature of the soil-pipeline interaction.

Figure 11a compares the deformed pipeline shape obtained with the analytical model and the measured deformation of the experimental pipeline for tests in dry sand. There is excellent agreement between the two, as well as close agreement between the analytical deformation and actual shape of the deformed pipeline as it was observed and documented after careful excavation. Figure 11b shows the measured and predicted strains under maximum ground deformation on both the compressive (extrados) and tensile (intrados) surfaces of flexure along the pipelines. The data point with an upward arrow indicates that strain gauges at the elbow reached the upper end of their measurement range at a time of rapidly increasing readings [16]. The maximum strain at the elbow, therefore, was larger than the value plotted. Overall, however, there is good agreement for both the magnitude and distribution of measured and analytical strains and deformation.

Once validated, the numerical modeling procedure was used to perform sensitivity studies in which various characteristics of the pipeline and elbow were varied to assess which would be most successful in reducing strain concentrations. It was found that increasing wall thickness by 33% in a small length of straight pipe welded to the elbow reduced strains by more than 70% [17].

(a) Pipeline Deformation After the Test   **(b) Distribution of Axial Strain**

Figure 11   Comparison Between Analytical and Experimental Results (Yoshizaki et al. [16])
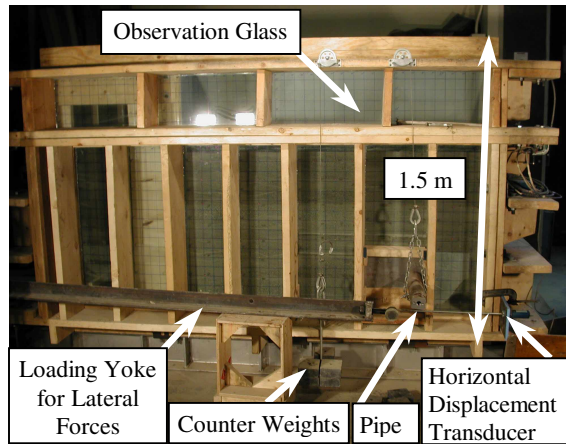
The large-scale experimental results also showed that lateral forces acting on the pipeline were greater for partially saturated sand than for dry sand. To explore the effects of partially saturated sand on the lateral force conveyed to buried conduits due to relative soil-pipe displacement, a series of additional tests were performed on pipe of similar size and composition. The tests were designed to be similar to those performed by Trautmann and coworkers [18, 19], who established design charts from which p-y relationships can be developed for analyzing pipe-soil interaction in response to lateral and vertical PGD.

These design charts were developed on the basis of experiments in dry sand. The great majority of pipelines in the field are embedded in partially saturated soils. Shear deformation of partially saturated sand mobilizes surface tension, or negative pore water pressure, that increases shear resistance relative to that in dry sand under comparable conditions of soil composition, in situ density, and loading. Moreover, the geometry of the failed soil mass for partially saturated sand is significantly different than the flow and displacement pattern of dry sand around buried pipe.
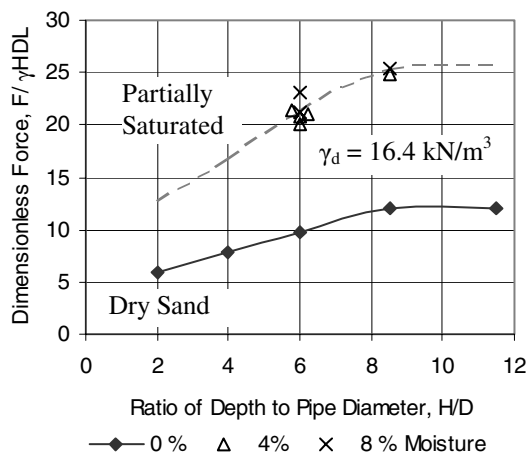
Figure 12 shows a photo of the test apparatus, which consisted of a box with interior dimensions 2.4 m × 1.2 m by 1.5 m deep. A special collar was fabricated to fit on top of the testing apparatus (not shown in the figure) that extended the depth of pipe burial to 2.3 m. Lateral force and displacement were conveyed to the pipe through a special yoke that allowed for unrestricted vertical movement as the pipe was displaced forward. Loads were applied by means of a hydraulic cylinder, and were measured with a calibrated load cell. A counterweight system was used to adjust the experimental pipe weight to be consistent with pipe weight in the field. Lateral and vertical pipe movements were measured with extensometers, and soil movements were measured by means of wooden dowels, embedded in the soil mass, which were visible through the glass sidewalls.

Sand similar to that used in the large-scale experiments with the pipeline-elbow assembly was placed in 150-mm lifts and compacted. Frequent in situ density and moisture content tests were performed. Dry unit weight and moisture content in the sand mass were controlled to within ±2% and ±5%, respectively. The sand was placed dry and at moisture contents of 4 and 8 %.
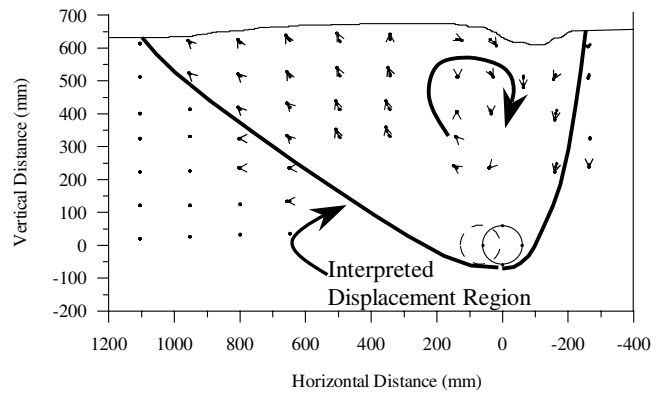
Figure 13 presents a plot of the dimensionless force, expressed as peak lateral load normalized by the product of total soil unit weight, pipe external diameter, length, and depth, versus the ratio of pipe depth to diameter. Values for partially saturated sand at 4 and 8% moisture plot along the same trend. The force associated with partially saturated sand is approximately twice that generated under dry sand conditions.
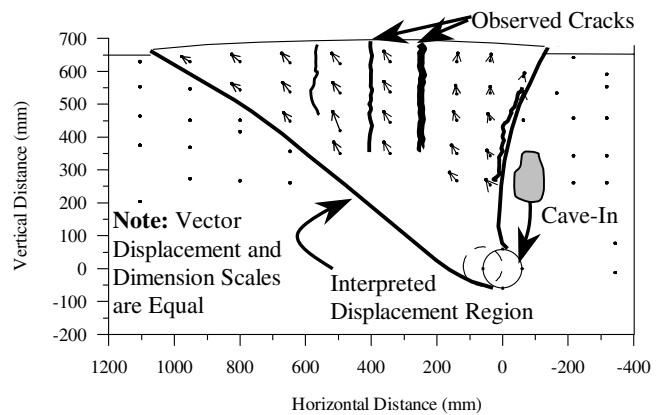
Figure 12   Experimental Facility for Full-scale Lateral Load-displacement of Buried Pipelines

(a) Dry Sand

Figure 13   Plot of Experimental Measurements for Lateral Forces Conveyed to Buried Pipe by Dry and Partially Saturated Sand

(b) Partially Saturated Sand

Figure 14   Soil Displacement Patterns for Dry and Partially Saturated Sand (after Turner [20])

Laboratory test results reported by Turner [20] show that increased shear resistance in partially saturated sand accounts only for about 30% of the increased lateral force relative to that for dry conditions. The principal cause of increased resistance can be explained with reference to Fig. 14, which shows the soil deformation patterns in dry and partially saturated sands. Dry sand deformation shows distinct zones of heave and subsidence, with continuous rotational movement between well-developed passive and active zones in front of and behind the pipe, respectively. In contrast partially saturated sand moves more like a coherent mass of soil that must be pushed forward and lifted by relative lateral movement of the pipe.

These experimental findings have important implications for lifeline design and construction. They confirm significantly increased lateral loads in partially saturated sand compared to those for dry sand that are currently used in practice [21]. The findings also illustrate the value of full-scale experiments, which were used to calibrate a general purpose analytical model, confirm higher reaction forces than predicted with current models, and point the way to a simple and effective means of reducing strain concentrations at elbows through moderate increases in the wall thickness of straight pipe sections adjoining the elbow.

In general, large-scale experiments play an essential role in discovering new mechanisms for soil and structural response, as well as key behavioral phenomena that were not previously appreciated. Such outcomes stimulate advances in modeling procedures.

As described elsewhere in these proceedings [22], substantial emphasis is being placed on the physical and numerical modeling of components with large and novel facilities, such as the George E. Brown, Jr. Network for Earthquake Engineering Simulation (NEES). This network is intended to unite a geographically dispersed system of equipment sites, users, modelers, and industrial partners through high performance Internet so that experiments at different sites can be coordinated, run, and numerically simulated at virtually the same time. Testing facilities for large displacement soil-structure interaction of lifeline components are being developed as part of NEES [22]. They provide a unique combination of large-scale and centrifuge modeling facilities. Large-scale testing duplicates pipe and soil behavior and the intricacies of soil-pipeline reactions. Centrifuge modeling provides an excellent complement, through which multi-g scaling is applied to extend the physical range of testing to larger prototype dimensions and rates of loading.

Lifeline systems, of course, are geographically distributed networks of components, which require an understanding of the spatial variability of component behavior and the integrated results of this variability with respect to system operation and community consequences. The treatment of lifeline performance is expanded in the next section to address issues related to system-wide variations in earthquake response.
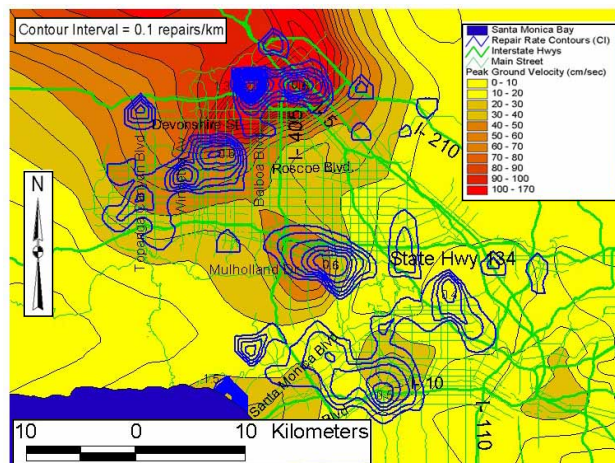
SPATIAL VARIABILITY OF EARTHQUAKE EFFECTS ON LIFELINES

Lifeline systems are large, geographically distributed networks that lend themselves to visualization and analysis with GIS. It is not surprising, therefore, that GIS has become an engine for driving new methodologies and decision support tools focused on the spatial variation of earthquake effects. GIS, for example, is the backbone of the National Loss Estimation Methodology sponsored by FEMA and implemented through HAZUS computer software [23, 24]. GIS also has been harnessed to explore the engineering and socioeconomic impacts of earthquakes through multidisciplinary studies of the losses incurred by disruptions of water supply and electric power systems [7, 25, 26, 27, 28, 29]. Advances in lifeline earthquake engineering have been influenced in a profound way by records of lifeline performance acquired after recent earthquakes, most notably the 1989 Loma Prieta, 1994 Northridge, 1995 Kobe, and 1999 Chi-chi earthquakes. Data from the Northridge, Kobe, and Chi-chi earthquakes have been compiled in GISs of unprecedented size and complexity that allow for a detailed examination of the spatial relationships among lifeline damage, permanent and transient ground deformation, and the surface, subsurface, and groundwater conditions.
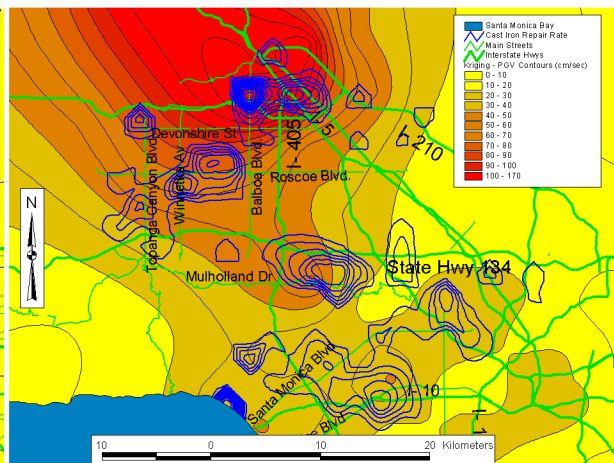
O'Rourke and Jeon [30, 31], for example, report on analyses of strong motion characteristics and their correlations with water supply pipelines and timber frame buildings conducted with very large GIS databases for the 1994 Northridge earthquake. GIS databases for water pipeline repair locations, characteristics of damaged pipe, and lengths of distribution (pipe diameter < 600 mm) and trunk (pipe diameter ≥ 600 mm) lines according to pipe composition and size were assembled with ARC/INFO software. Nearly 10,000 km of distribution lines and over 1,000 km of trunk lines were digitized.

Figure 15 presents a map of distribution pipeline repair locations and repair rate contours for cast iron pipeline damage superimposed on peak ground velocity (PGV) zones. The repair rate contours were developed by dividing the map into 2 km × 2 km areas, determining the number of cast iron pipeline repairs in each area, and dividing the repairs by the distance of cast iron mains in the area. The PGV zones were developed by interpolating the larger of the two horizontal components associated with each of 164 corrected strong motion records. Using the GIS database, a pipeline repair rate was calculated for each PGV zone, and regression analyses were performed to determine a relationship between pipeline repair rate and average PGV [32, 33].

Figure 15   Map of PGV Estimated by TIN on Contours of Cast Iron Pipeline Repair Rates (after O'Rourke and Toprak [32])

Figure 16   Map of PGV Estimated by Kriging on Contours of Cast Iron Pipeline Repair Rates (after Jeon [33])
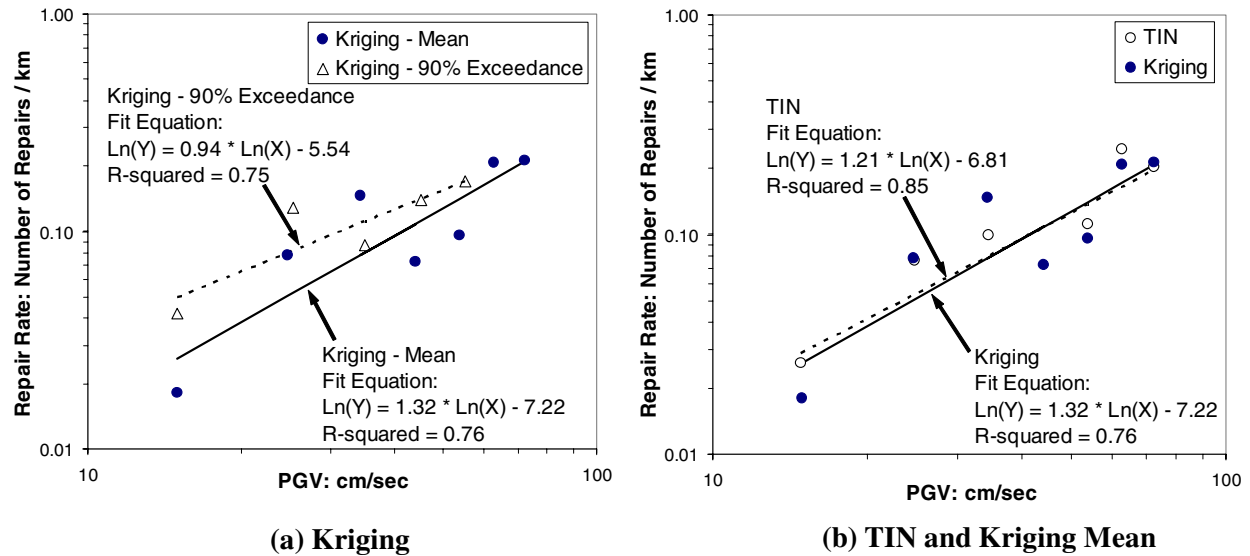
The interpolation of PGVs from strong motion recording sites was performed by Triangulated Irregular Network (TIN) techniques implemented in the ARC/VIEW software. This type of interpolation process provides no statistical measure of uncertainty. Regression analyses for predicting pipeline damage without statistical procedures are based by default on the assumption that seismic parameters are known without error and that any statistical measure of uncertainty will apply only for pipeline repair rates.

To investigate the spatial variability of PGV, ordinary kriging was performed. Ordinary kriging is a geostatistical process for making unbiased estimates at unsampled locations with the smallest estimates of variance [34, 35]. It does so by quantifying the spatially correlated variance of the difference in seismic parameters at all sampled locations in the form of a variogram. The variogram is then used to make weighted average estimates at unsampled locations from neighboring recorded values. One of the great strengths of ordinary kriging is that it provides a statistical measure of uncertainty for estimated seismic parameters.

It is frequently assumed that seismic parameters are log (ln) normally distributed. To confirm the appropriate model for the distribution of PGV, values from 164 records of Northridge earthquake strong motion were used to develop a cumulative frequency distribution for goodness-of-fit testing using the Kolmorgorov-Smirnov (K-S) test. Cumulative frequency distributions were constructed for both the arithmetic and ln values of PGV. It was found that there is a significantly better agreement between the K-S theoretical distribution [F(x)] and observed cumulative frequency [Fn(x)] plot for ln(PGV). In addition, the Cressie goodness of fit statistic [36] was calculated to show that a spherical variogram model was appropriate for characterizing the variance of PGV at two different sites as a function of the distance separating them.

With the appropriate statistical distribution model and variogram representation, ordinary kriging was applied to the PGV data to produce the PGV zones illustrated in Fig. 16. Cast iron pipeline repair rate contours are superimposed on the PGV zones. A close comparison between Figs. 15 and 16 shows that the spatial distribution of PGV from TIN techniques and kriging are similar. The main advantage of kriging is that it provides the means for quantifying uncertainty about PGV at any given location.

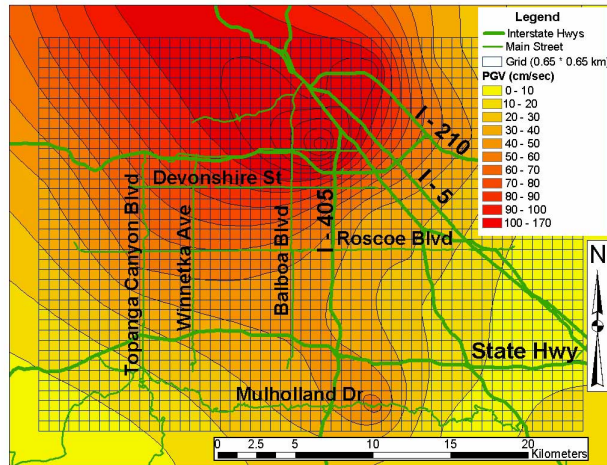**Figure 17   Cast Iron Pipeline Repair Rate vs PGV Determined by Kriging and TIN (Adapted from Jeon [33])**

Applying standard statistical techniques, the PGV values corresponding to 90% exceedance were calculated for locations throughout the water distribution network. Such values leave only a 10% chance that a lower value may have actually influenced a particular location during the Northridge earthquake. This type of characterization allows one to compensate for the spatial variability of the data and make predictions with higher confidence than those forecast on the basis of mean values.

Figures 17 a and b present linear regressions of cast iron pipeline repair rates versus PGV representing mean and 90% exceedance values for ln(PGV). As can be seen in Fig. 17a, the 90% exceedance values plot higher than the mean, and thus provide a higher degree of confidence that predictions won't underestimate the actual repair rate because the estimated ground motion inferred from the GIS database was too high. Figure 17b shows that the regressions based on TIN interpolation and kriging are very close, consistent with visual inspection of PGV zones in Figs. 15 and 16.
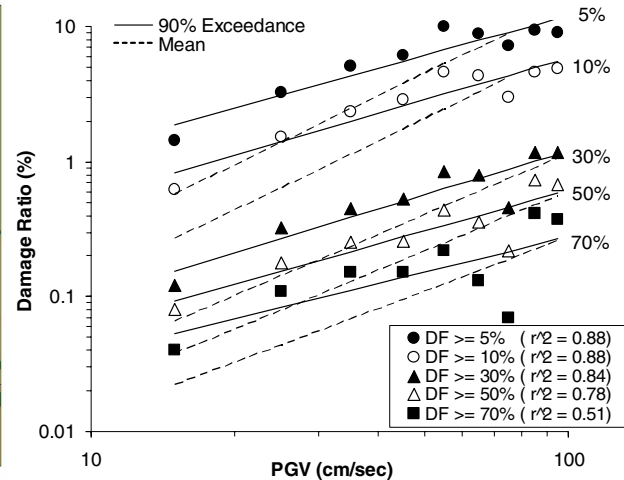
The statistical procedures for characterizing spatial variability of ground motion for empirical models to predict pipeline damage can also be applied to aboveground structures. O'Rourke and Jeon [31] report on how safety inspection records were collected for 47,378 one- and two-story timber buildings that were inspected by structural engineers after the 1994 Northridge earthquake. The inspection records include information about number of stories, estimated age, estimated damage as a percentage of replacement cost, and the latitude and longitude of each inspected building.

Data about the number of existing timber buildings were also obtained from 1994 tax assessor records acquired in disaggregated form from information compiled by the California Office of Emergency Services (OES). The total number of existing structures in this data set is 278,662. The data were provided for GIS evaluation as the number of buildings within each of 2106 cells that were arranged as a grid covering the San Fernando Valley area.

These data sets were used to evaluate relationships among timber building damage after the 1994 Northridge earthquake and various seismic parameters, including PGV. Two damage parameters, referred to as damage ratio and damage factor, were calculated. Damage ratio is the fraction or percentage of existing structures with damage equal to or exceeding a particular damage factor. Damage factor is damage expressed as a percentage of building replacement cost.

Figure 18   GIS Grid with Tax Assessor Data Superimposed on PGV Determined by Kriging

Figure 19   Damage Ratio Regression for 90% Exceedance and Mean PGV (after Jeon [33])

The number of residential timber structures was geocoded at the center of each 0.65 km x 0.65 km cell in the GIS database, and the PGVs estimated at various exceedance levels were determined from the 164 strong motion records. Figure 18 shows the GIS grid superimposed on the spatial variation of mean PGV determined by kriging. By using a grid in which each cell is characterized by various damage ratios linked with damage factors, linear regressions were developed to quantify damage vs. seismic parameters for loss estimation purposes.
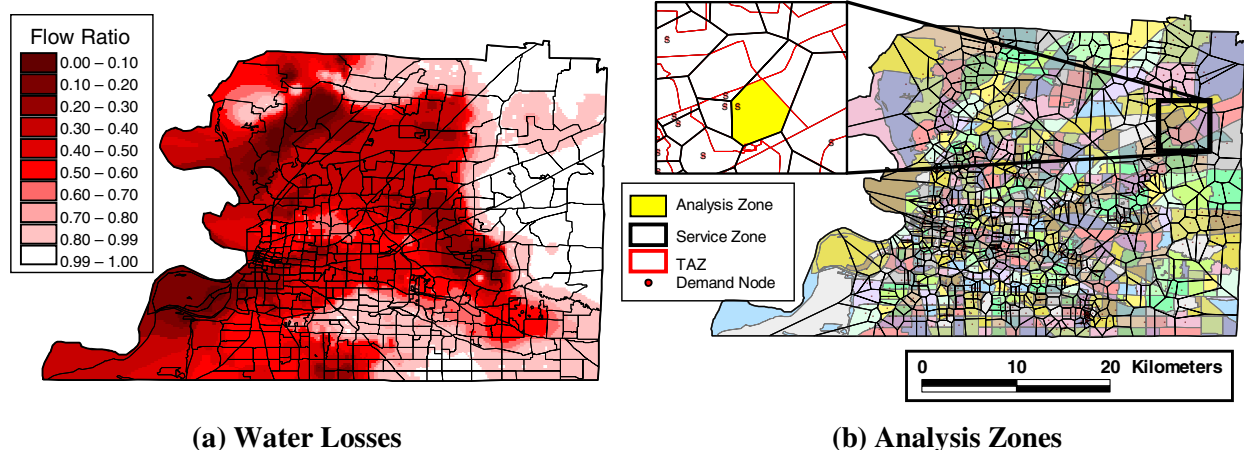
Regressions were developed according to the same procedure used for the cast iron water mains. Figure 19 shows the damage ratio versus PGV for mean and 90% exceedance values as well as various values of damage factor, DF. Data points are plotted only for the 90% exceedance values. Most regressions for PGV show very good fits as indicated by high r^2 values, with the exception of DF $\geq$ 70%. As expected, the regressions for the 90% exceedance values plot above those for mean PGV.

The research also showed that Seismic Intensity is the damage predictor most statistically significant for timber buildings. Seismic Intensity is defined as the weighted average pseudo-velocity, obtained from the response curve for a damping ratio of 20% between periods of 0.1 and 2.5s [31]. The methodology is thus able to identify parameters best suited for loss estimation.

The capabilities that are available with the current generation of GIS software provide the means of evaluating the spatial variability of seismic hazards, system characteristics, and system response. These features may be thought of as databases that are part of physical infrastructure. When spatially variable databases of this type are combined with social and economic data sets (representing social infrastructure), then the regional consequences for communities of lifeline system response to earthquakes can be explored. Recent work in which lifeline system response has been related to regional economic consequences are discussed in the next section.

REGIONAL ECONOMIC AND SOCIAL CONSEQUENCES

Lifelines are interwoven with the fabric of the communities they serve. Measures for assessing the effects of lifeline earthquake damage should therefore quantify lifeline losses in terms of regional economic and social impacts. Water supply damage, for example, adversely affects fire protection, the loss of which triggers serious local cost and regional economic reactions. Lifeline system disruption has

(a) Water Losses   **(b) Analysis Zones**

Figure 20   GIS and Seismic Zonation for Assessing the Economic Effects of Lifeline Losses in Shelby County, TN (after Chang et al. [28])

a direct effect on business losses that, in turn, have multiple related effects on other businesses. There is a growing body of research and applications associated with the economic and social consequences of lifeline damage and loss of functionality. Several examples are described in this paper to illustrate promising developments and show the direction of future advances in lifeline earthquake engineering.

Accounting for Spatial Variability in Economic Assessment

Chang et al. [27] illustrate how disruption in water delivery caused by lifeline earthquake damage affects the regional economy, and describe methods for dealing with the spatial variability of economic impacts. Their work focuses on the water distribution system of Memphis Light, Gas, and Water (MLGW) in Shelby County, TN and its potential response to earthquakes originating in the New Madrid Seismic Zone. The methodology involves the evaluation of individual earthquake scenarios for events with different magnitudes and distances. For each scenario earthquake, Monte Carlo simulations are performed during which earthquake effects are modeled.

For the MLGW water distribution system, damage states were evaluated with a hydraulic network model configured for the piping and facilities operated by MLGW. For each earthquake scenario, 100 cases of simulated system-wide damage were produced. Figure 20a shows the ratio of water flow in the damaged system, averaged over the 100 simulations, to water flow in the undamaged system for a 7.0 M_w earthquake at Marked Tree, AR. The water flow and associated damage states are those that immediately follow the earthquake.

Economic data for various areas of the U.S. are summarized according to census tracts, which are divisions of land that are designed to contain 2,500 to 8,000 inhabitants with relatively homogeneous population characteristics, economic status, and living conditions. There are 133 census tracts in Shelby County. To provide a finer grain for economic analysis, Traffic Analysis Zones (TAZs) were used. There are 515 TAZs for Shelby County that contain information on local employment. Such zones represent aggregated census data developed jointly by the U.S. Bureau of Census and U.S. Department of Transportation.

Figure 20b shows how analysis zones were created by overlaying 515 TAZs with 685 water service zone polygons. GIS Thiessen polygons [34] were generated to represent the inferred service areas for all demand nodes in the water delivery system. Assuming that there is a uniform labor distribution within each industry, the employment data for each TAZ can be linked with economic output. The amount of economic output in each TAZ affected by water losses was estimated as being directly proportional to the

fraction of the TAZ overlapped by a polygon. In this way the economic activity and water losses in Shelby County were correlated in 2,784 analysis zones, thereby providing a spatial framework for the distribution of lifeline damage effects on the regional economy.

The analysis zones provide modeling advantages over other spatial aggregates of data, such as census tracts, which are not related to the water network topology and are relatively large spatial units. The analysis zones are relatively small areas that provide better spatial definition for economic assessment. Moreover, they are structured with explicit recognition of the water supply nodes.
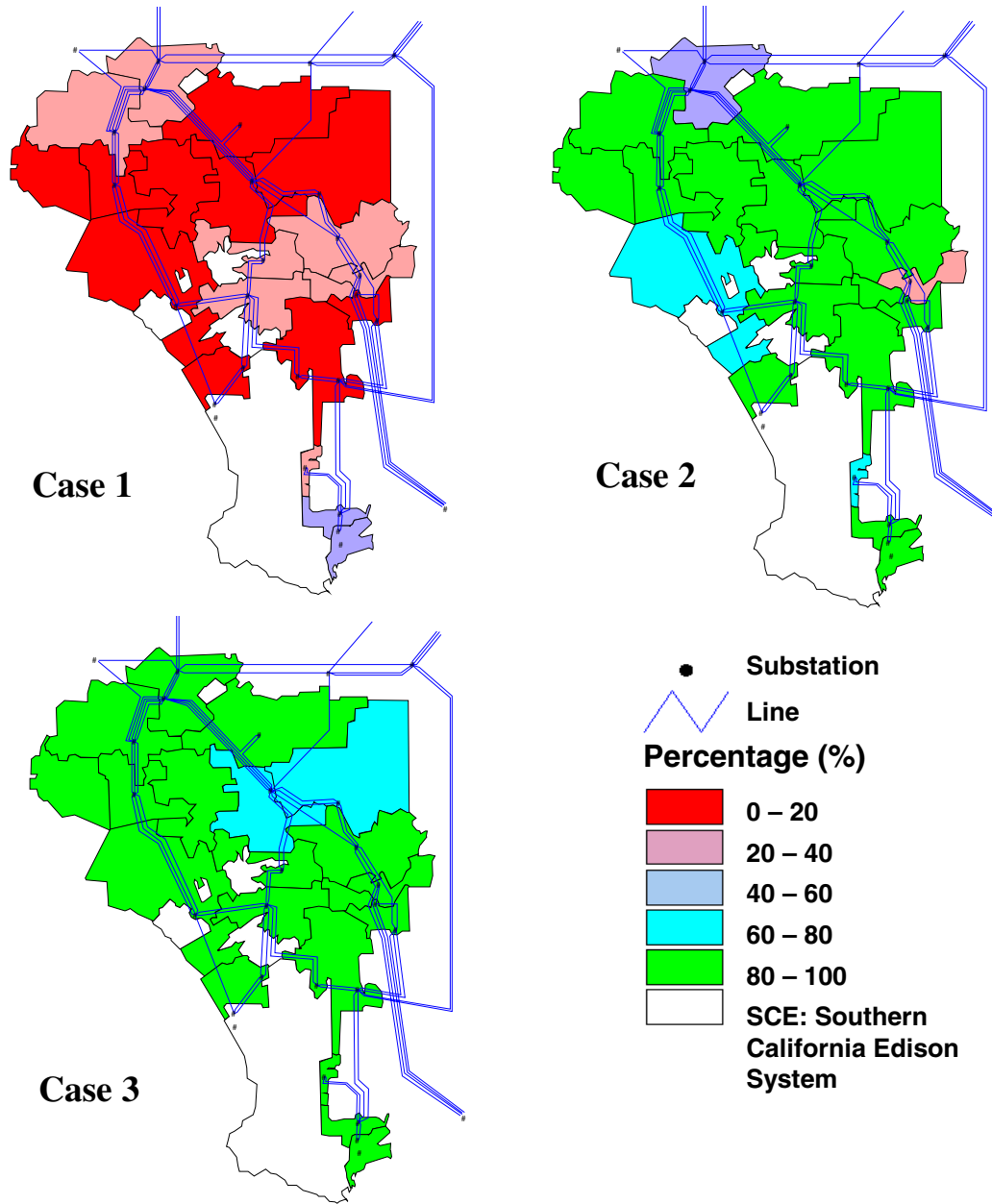
Using business surveys conducted in Memphis and in Los Angeles after the 1994 Northridge earthquake [37, 38], empirical factors were developed to represent resilience in economic loss modeling. A "resiliency factor" is defined as the remaining percentage output that a given industry could produce in the event of total water loss. An economic loss model, which incorporates resilience, was implemented by means of Monte Carlo simulations. In each simulation, an assessment of economic output for each of 16 industries in each of the 2,784 analysis zones in weekly time periods was made. Loss factors, calculated for the analysis zones, were converted to dollar losses, and integrated to estimate the direct business loss resulting from earthquake damage of the water supply network. An evaluation of various retrofitting options was performed on the economic loss predictions as the means for deciding on the best rehabilitation measures. Structural and operational improvements of groundwater well pumping stations were shown to be the best retrofitting strategy to reduce regional economic consequences.

Accounting for System Performance Criteria

Methodologies for evaluating the post-earthquake performance of electric power systems have been developed and applied to the Los Angeles area by Shinozuka and Chang [7]. Of particular interest is the work that explores the effects of component performance on the system-wide behavior of the Los Angeles electric power network after earthquakes. Modeling of the LADWP power transmission network was performed with the software IPFLOW, available through the Electric Power Research Institute (EPRI). Full-scale experiments were performed on electric power transformers to evaluate improvements in seismic performance associated with base isolation [39]. Moreover, performance data for LADWP transformers compiled after the Northridge earthquake were used to develop fragility curves for transformers in the form of a two-parameter (median and log-standard deviation) lognormal distribution, as a function of peak ground acceleration, PGA. By using the experimental data related to base isolation, improvements in transformer performance were accounted for by means of an enhancement index.

Power flow analyses were performed for a suite of 47 scenario earthquakes, compiled to represent the seismic hazard for the LADWP electric power system. The analyses were performed 20 times for each scenario earthquake. Figure 21 shows the ratio of mean power supply in the damaged network to that of the undamaged network for each LADWP service area for a scenario earthquake (based on a M_w 7.3 Malibu Coast earthquake) where only transformers are considered vulnerable. The mean is taken over the entire sample, which includes the 20 power simulations. The figure illustrates system behavior in terms of power supply ratio for various degrees of enhanced transformer performance, corresponding to Cases 1, 2, and 3 for no retrofit, 50% enhancement, and 100% enhancement, respectively. The steady improvement in power flow can be seen as transformer response is improved from Case 1 to 3.
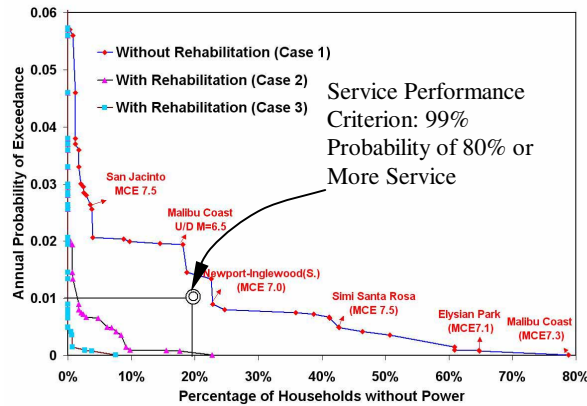
Figure 22 presents risk curves derived from the system simulation and 47 scenario earthquakes, for which the annual probability of exceedance is plotted relative to the percentage of households lacking electricity immediately after an earthquake. The risk curves are plotted for Cases 1 through 3. The risk curve format provides a rational means for linking system performance criteria with component improvement. For example, if the performance criterion is specified as an annual probability of 0.99 that
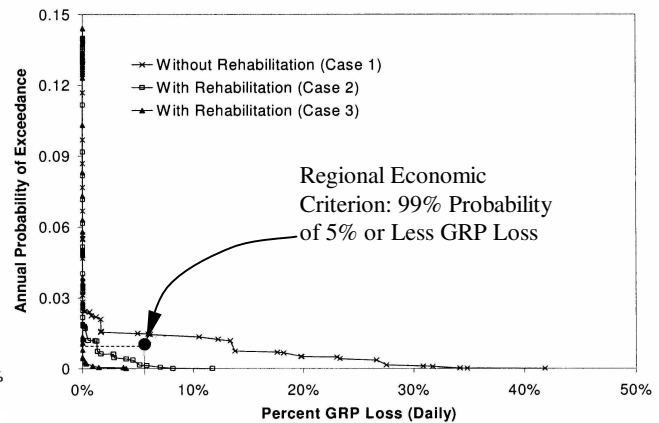
Figure 21   Relative Average Power Output for LADWP System with Only Transformers Vulnerable (after Shinozuka and Chang [7])

80% or more households will have power immediately after any earthquake, that requirement can be viewed in context of the risk curve. The criterion is plotted as the doubled circle point in Fig. 22. The risk curve for Case 1 (without retrofitting) does not satisfy this criterion, but the risk curves for Cases 2 and 3 (with retrofitting) do.

Shinozuka and Chang [7] also adapted the spatial loss of electric power to its regional economic consequences in terms of direct business losses in dollars. Business losses were estimated using the same survey data [37] that were applied to water supply effects previously discussed, as well as additional information sources and procedures. Loss results are presented in Fig. 23 as the percent of gross regional product (GRP) in the LADWP service area that would be lost given the electric power outage in each

Figure 22   Risk Curves for Household Power Outage (after Shinozuka and Chang [7])

Figure 23   Risk Curves for Economic Loss (after Shinozuka and Chang [7])

simulation earthquake. The results are assessed in terms of daily GRP loss. A regional economic criterion, pertaining to 0.99 probability that losses do not exceed 5% GRP from any earthquake, is plotted relative to the economic risk curves. Case 1 for this criterion does not meet the performance standard, however Cases 2 and 3 do.

Economic Models

The direct regional economic consequences of lifeline loss will, in turn, have indirect economic effects. A factory, for example, may have electric power. If one of its key supplies, however, is not operating due to electricity losses sustained in another part of the system, factory productivity will decline. The total economic effect will be a multiplier of the direct loss.

Indirect economic losses generated by seismic damage to lifelines were initially estimated with Input-Output (I-O) analysis [40, 41], which is based on tabulated economic data pertaining to purchases (inputs) and sales (outputs) among all sectors of the regional economy. The model is based on the assumption that a linear relationship exists between inputs and outputs. Recent modeling employs the Computable General Equilibrium (CGE) method [42] to assess losses. This method incorporates nonlinear interactions through multi-market simulation models that optimize the behavior of consumers.

I/O models simplify general economic equilibrium into interdependencies among sectors that are unidirectional and removed from the offsetting effects of price reduction. They do not allow for adaptive behavior, such as conservation of resources or substitution of alternative supplies. As such, it is not uncommon for I-O models to yield multiplier effects that are more than double the direct losses.

As Rose and Liao [42] point out CGE models provide a more accurate representation of economic forces as well as the interplay among sectors of the regional economy. CGE models are nonlinear and readily incorporate adaptive responses, such as conservation and substitution. They can account for seismic resilience, and their results provide for lower, more realistic estimates of economic impacts than those of I-O models. GCE models are currently being applied to evaluate the indirect, regional consequences of water supply loss in Portland, as well as both electric power and water supply losses from earthquakes in Los Angeles [42].

Lifeline systems are built over many years, and the majority of network components are expected to function for long periods of time. It is important, therefore, to evaluate retrofitting alternatives under a life cycle cost framework. Shinozuka et al. [39] describe a methodology for evaluating various earthquake

mitigation strategies in terms of total life cycle costs, including utility revenue losses, cost of repairs, and regional economic impact from loss of lifeline services. Total life cycle cost is calculated as the cost of seismic mitigation plus the sum of the annualized expenses for earthquake repair, loss of revenue after an earthquake, and direct regional economic losses that accrue over a benchmark time period. Their evaluations of the life cycle costs of retrofitting electric power transformers for the LADWP system show that seismic mitigation expenses exceed the reduction in losses if only lost revenue and repair costs are considered. If, however, the direct regional economic consequences are taken into account, the life cycle savings far exceed the mitigation expenses. Moreover, the cost-effectiveness of seismic protection increases further if indirect economic effects are factored into the assessment.

CONCLUDING REMARKS

Advances in lifeline earthquake engineering are generated increasingly by system-wide evaluations to quantify service reliability and estimate the consequences of service disruptions on both the economy of a given region and its social networks. A framework is provided in this paper for evaluating lifeline system performance with the goal of enhancing the seismic resilience of communities. The framework is structured around a basic chain of activities that includes the characterization of seismic hazards and system properties, analyses of the interaction between seismic demand and lifeline component or facility response, and the assessment of system response and its consequences for the regional economy and community institutions. The framework is applicable to hazards other than earthquakes, including natural and anthropogenic ones. Considerable benefit, in fact, can be derived from lifeline earthquake engineering for improving the security of civil infrastructure from natural hazards as well as major accidents and premeditated acts of violence.

Using the framework for lifeline systems assessment, the paper explores various aspects of systems performance and modeling. It provides an example of component modeling, using jointed concrete cylinder pipelines (JCCPs), which are important trunk and transmission pipelines in North American water supplies. A model for seismic wave interaction with JCCPs is explained, which expands on empirical models derived by calculating pipeline repair rates after previous earthquakes with measured peak ground velocities. A dimensionless plot is developed to estimate JCCP joint deformation as a function of soil conditions, key pipeline properties, and seismic wave characteristics.

Permanent ground deformation (PGD) is the most important seismic hazard for underground facilities, and select results are presented of recent large-scale experiments to characterize PGD effects on natural gas pipelines with elbows. The paper also presents the results of recent full-scale experiments, which show that the lateral forces imposed on pipelines by partially saturated sand are approximately twice as large as those generated by dry sand. These findings have significant repercussions for design/construction in that the current generation of analytical models is based on lateral force-displacement relationships for dry sand. Thus, the new experimental results will allow for more realistic modeling, and will reflect the actual in situ moisture conditions affecting the great majority of underground lifelines.

The spatial variability of strong ground motion and its effects on water supply performance are examined with reference to large GIS databases compiled after 1994 Northridge earthquake. A methodology is presented for using ordinary kriging in combination with GIS to obtain confidence limits on the strong motion used for empirical models that correlate pipeline repair rate with seismic parameters. The geostatistical procedures used for pipelines are shown to apply equally well for aboveground structures. The paper describes how the methodology is applied for loss estimation modeling of earthquake damage to timber residential buildings.

The paper provides a review of recent work focused on quantifying lifeline losses in terms of regional economic and social impacts. Procedures are explained that account for the spatial variability of earthquake economic consequences by reference to work performed for the water distribution system in Memphis, TN. The paper explains how risk curves for system response to earthquakes can be used with performance criteria for both service and regional economic impacts by reference to work performed for the electric power transmission system in Los Angeles, CA.

Both the direct and indirect economic consequences of earthquake damage in lifeline systems are discussed. Computable General Equilibrium models are shown to be preferable to Input-Output models for assessing the indirect economic effects of lifeline losses.

Life cycle cost analysis is also discussed. It is highly recommended that decision support tools account for direct and indirect regional economic consequences to provide ground truth for planning and implementing earthquake mitigation procedures.

ACKNOWLEGEMENTS

REFERENCES

1. O'Rourke, T.D., "An Overview of Geotechnical and Lifeline Earthquake Engineering." Geotechnical Special Publication No. 75, ASCE, Reston, VA, Proceedings of Geotechnical Earthquake Engineering and Soil Dynamics Conference, Seattle, WA, Aug. 1998, Vol. 2, pp.1392-1426.
2. O'Rourke, T.D., Lembo, A.J., and Nozick, L.K., "Lessons Learned from the World Trade Center Disaster About Critical Utility Systems." Beyond September 11th: An Account of Post-disaster Research, Program on Environment and Behavior Special Publication #39, Natural Hazards Research and Information Center, University of Colorado, Boulder, CO, April, 2003, pp. 269-290.
3. Wallace, W.A., Mendonca, D., Lee, E.E., Mitchell, J.E. and Chow, J.H., "Managing Disruptions to Critical Interdependent Infrastructures in the Context of the 2001 World Trade Center Attack." Beyond September 11th: An Account of Post-disaster Research, Program on Environment and Behavior Special Publication #39, Natural Hazards Research and Information Center, University of Colorado, Boulder, CO, April, 2003, pp. 165-198.
4. Zimmerman, R., "Public Infrastructure Service Flexibility for Response and Recovery in the Attacks at the World Trade Center, September 11, 2001." Beyond September 11th: An Account of Post-disaster Research, Program on Environment and Behavior Special Publication #39, Natural Hazards Research and Information Center, University of Colorado, Boulder, CO, April, 2003, pp. 241-268.

5. Bruneau, M., Chang, S.E., Eguchi, R.T., Lee, G.C., O'Rourke, T.D., Reinhorn, A.M., Shinozuka, M., Tierney, K., Wallace, W.A., and Winterfeldt, D., "A Framework to Quantitatively Assess and Enhance the Seismic Resilience of Communities." Earthquake Spectra, Vol. 19, No. 4, Nov. 2003, pp.733-752.

6. Bird, J., O'Rourke, T.D., Bracegirdle, A., Bommer, J. and Tromans, I., "A Framework for Assessing Earthquake Hazards for Major Pipelines." Proceedings of the International Conference on Terrain and Geohazards Facing Onshore Oil and Gas Pipelines, London, UK, June, 2004.

7. Shinozuka, M. and Chang, S.E., "Evaluating the Disaster Resilience of Power Networks and Grids." Modeling Spatial Economic Impacts of Disasters, Springer-Verlag, Edited by Y. Okuyama and S.E. Chang, 2004(in press).

8. Ayala, A. G. and O'Rourke, M. J., "Effects of the 1985 Michoacan Earthquake on Water System and Other Buried Lifelines in Mexico City." Technical Report NCEER-89-0009, MCEER, Buffalo, NY, Mar. 1989.

9. Lund, L., "Water System." Northridge Earthquake Lifeline Performance and Post-Earthquake Response, Edited by A. J. Schiff, TCLEE Monograph No. 8, ASCE, NY, Aug. 1995, pp. 96-131.

10. O'Rourke, T.D., Wang, Y., Shi, P., and Jones, S., "Seismic Wave Effects on Water Trunk and Transmission Lines." Proceedings of the 11th International Conference on Soil Dynamics & Earthquake Engineering, and 3rd International Conference on Earthquake Geotechnical Engineering, Berkeley, CA, Jan. 7-9, 2004, Vol. 2, pp. 420-428.

11. O'Rourke, T.D. and Jeon, S-S., "Seismic Zonation for Lifeline and Utilities." Proceedings of the 6th International Conference on Seismic Zonation, Palm Springs, CA, Nov. 2000, EERI, Oakland, CA.

12. O'Rourke, T.D., Stewart, H.E., and Jeon, S-S., "Geotechnical Aspect of Lifeline Engineering." Proceedings of the Institution of Civil Engineers, Geotechnical Engineering, Vol. 149, Issue 1, Jan. 2001, pp. 13-26.

13. Wu, C., Fok, E., Fotinos, G., Tseng, W., and Oberholtzer, G., "Seismic Assessment and Retrofit Concepts of the BART Transbay Tube." Proceedings of the 6th US Conference and Workshop on Lifeline Earthquake Engineering, Long Beach, CA, TCLEE Monograph No. 25, ASCE, Reston, VA, Aug., 2003, pp. 203-212.

14. O'Rourke, M.J. and Liu, X., "Response of Buried Pipelines Subject to Earthquake Effects." Multidisciplinary Center for Earthquake Engineering Research, Monograph Series No. 3, Buffalo, NY, 1999.

15. Eidinger, J.M., O'Rourke, M., and Bachhuber, J., "Performance of a Pipeline at a Fault Crossing." Proceedings of the 7th National Conference on Earthquake Engineering, Boston, MA, July, 2002, EERI, Oakland, CA.

16. Yoshizaki, K., O'Rourke, T.D., and Hamada, M., "Large Scale Experiments of Buried Steel Pipelines with Elbows Subjected to Permanent Ground Deformation." Journal of Structural Mechanics and Earthquake Engineering, JSCE, Tokyo, Japan, Vol. 20, No. 1, Jan. 2003, pp. 1-11.

17. Yoshizaki, K., "Study on Large Deformation Behavior of Buried Pipelines with Elbows Subjected to Permanent Ground Deformation." Ph.D. Dissertation, Waseda University, Tokyo, Japan, Mar. 2002.

18. Trautmann, C.H. and O'Rourke, T.D., "Lateral Force-Displacement Response of Buried Pipe." Journal of Geotechnical Engineering, ASCE, Reston, VA, Vol. 111. No. 9, 1985, pp. 1068-1084.

19. Trautmann, C.H., O'Rourke, T.D. and Kulhawy, F.H., "Uplift Force-Displacement Response of Buried Pipe." Journal of Geotechnical Engineering, ASCE, Vol. 111, No. 9, 1985, pp.1061-1067.

20. Turner, J.E., "Lateral Force Displacement Behavior of Pipes in Partially Saturated Sand." Master of Science Thesis, Cornell University, Ithaca, New York, May 2004.

21. Committee on Gas and Liquid Fuel Lifelines of the ASCE Technical Council on Lifeline Earthquake Engineering, "Guidelines for the Seismic Design of Oil and Gas Pipeline Systems." ASCE, Reston, VA, 1984.

22. Jones, S.L., Kesner, K.E., O'Rourke, T.D., Stewart, H.E., Abdoun, T., and O'Rourke, M.J., "Soil-Structure Interaction Facility for Lifeline Systems." Proceedings of the 13th World Conference on Earthquake Engineering, Vancouver, BC, Canada, Aug., 2004, Paper No. 1621.

23. National Institute of Building Sciences, Earthquake Loss Estimation Methodology HAZUS 97: Technical Manual, prepared for Federal Emergency Management Agency, Washington, D.C., 1997.
24. Whitman, R.V., Anagnos, T., Kircher, C.A., Lagorio, H.J., Lawson, R.S., and Schneider, P., "Development of a National Earthquake Loss Estimation Methodology." Earthquake Spectra, EERI, Oakland, CA, Vol. 13, No. 4, 1997, pp. 643-661.
25. Chang, S.E., Seligson, H.A., and Eguchi, R.T., "Estimation of the Economic Impact of Multiple Lifeline Disruption: Memphis Light, Gas and Water Division Case Study." Technical Report NCEER-96-0011, National Center for Earthquake Engineering Research, State University of New York at Buffalo, Buffalo, NY, 1996.
26. Shinozuka, M., and Hwang, H.H.M., "Seismic Performance of Electric Power System." Engineering and Socioeconomic Impacts of Earthquake: An Analysis of Electricity of Lifetime Distributions in New Madrid Area, Multidisciplinary Center for Earthquake Engineering Research, Monograph Series No. 2, Buffalo, NY, 1998, pp. 33-43.
27. Chang, S.E., Svekla, W.D., and Shinozuka, M., "Linking Infrastructure and Urban Economy: Simulation of Water Disruption Impacts in Earthquakes." Environment and Planning B, Vol. 29, No. 2, 2002, pp. 281-301.
28. Chang, S.E., "Transportation Planning for Disasters: An Accessibility Approach." Environment and Planning A, Vol. 35, 2003, pp. 1051-1072.
29. Kakumoto, S., Hatayama, M., and Kameda, H., "Advanced GIS Applications for Earthquake Disaster Mitigation." Proceedings of the 1st MCEER Workshop on Mitigation of Earthquake Disaster by Advanced Technologies, MCEER, Buffalo, NY, 2000, pp. 211-216.
30. O'Rourke, T.D. and Jeon S.-S., "Factors Affecting the Earthquake Damage of Water Distribution Systems." Proceedings of 5th US Conference on Lifeline Earthquake Engineering, Seattle, WA, TCLEE Monograph No. 16, ASCE, Reston, VA, Aug. 1999, pp. 379-388.
31. O'Rourke, T.D. and Jeon S.-S., "GIS Loss Estimation and Post-Earthquake Assessment of Residential Building Damage." Proceedings of the 7th National Conference on Earthquake Engineering, Boston, MA, July, 2002, EERI, Oakland, CA.
32. O'Rourke, T.D., and Toprak, S., "GIS Assessment of Water Supply Damage from the Northridge Earthquake." Geotechnical Special Publication No. 67, Frost, J.D. Ed, ASCE, Reston, VA, 1997, pp. 117-131.
33. Jeon S.-S., "Earthquake Performance of Pipelines and Residential Buildings and Rehabilitation with Cast-in-Place Pipe Lining Systems." Ph.D. Dissertation, School of Civil & Environmental Engineering, Cornell University, Ithaca, NY, 2002.
34. Burrough, P. A. and McDonnell, R. A., Principles of Geographical Information Systems, Oxford University Press, Oxford, England, 1998.
35. Clark, I. and Harper, W. V., Practical Geostatistics 2000, Ecosse North America Llc, Columbus, OH, 2000.
36. Cressie, N.A.C., Statistics for Spatial Data, John Wiley & Sons, Inc., Revised Edition, NY, 1993.
37. Tierney, K.J., "Business Impacts of the Northridge Earthquake." Journal of Contingencies and Crisis Management, Vol. 5, 1997, pp. 87-97.
38. Tierney, K.J. and Dahlhamer, J.M., "Earthquake Vulnerability and Emergency Preparedness Among Businesses." Engineering and Socioeconomic Impacts of Earthquake: An Analysis of Electricity of Lifetime Distributions in New Madrid Area, Multidisciplinary Center for Earthquake Engineering Research, Monograph Series No. 2, Buffalo, NY, 1998, pp. 53-74.
39. Shinozuka, M., Feng, M., Dong, X., Chang, S.E., Cheng, T.-C., Jin, X., and Ala Saadeghvaziri, M., "Advances in Seismic Performance Evaluation of Power Systems." Research Progress and Accomplishments 2001-2003, Multidisciplinary Center for Earthquake Engineering Research, Buffalo, NY, 2003, pp. 1-16.

40. Rose, A., Benavides, J., Chang, S., Szczesniak, P., and Lim, D., "The Regional Economic Impact of an Earthquake: Direct and Indirect Effects of Electricity Lifeline Disruptions." Journal of Regional Science, Vol. 37, Issue 3, 1997, pp. 437-458.
41. Rose, A. and Lim, D., "Business Interruption Losses from Natural Hazards: Conceptual and Methodological Issues in the Case of the Northridge Earthquake." Environmental Hazards, Vol. 4, 2002, pp.1-14.
42. Rose, A. and Liao, S-Y., "Understanding Sources of Economic Resiliency to Hazards: Modeling the Behavior of Lifeline Service Customers." Research Progress and Accomplishments 2001-2003, Multidisciplinary Center for Earthquake Engineering Research, Buffalo, NY, 2003, pp. 149-160.